RSC Advances

PAPER

View Article Online
View Journal | View Issue

Cite this: *RSC Adv.*, 2025, **15**, 6952

The preparation of titanium adipate and optimization of its catalytic ester exchange reaction for the synthesis of diisooctyl adipate

Linlin Zhao, Guoliang Shen, * Tiejun Xu, Ruiyang Wen and Sijin Jiang

Chelated titanium adipate with stable properties was prepared *via* an ester-exchange reaction using low-carbon alkyl titanate, and it was characterized and analyzed using infrared spectroscopy, thermogravimetry, and scanning electron microscopy. Diisooctyl adipate (DOA) was synthesized *via* an ester-exchange method using the synthesized novel titanium adipate as a catalyst and isooctanol and dimethyl adipate as raw materials, where dimethyl adipate is the methyl esterification product of the by-product (mixed dicarboxylic acid) in industrial adipic acid production. The process is easy to carry out, green and environmentally friendly, and the methanol by-product can be recycled and utilized. With the objective of optimizing the DOA ester exchange rate, the effects of three factors, namely, catalyst dosage, the molar ratio of isooctanol to dimethyl adipate and the reaction temperature at catalyst addition, on the optimization objective were systematically investigated *via* one-way and response surface tests. Analysis of variance (ANOVA) and parameter optimization were conducted using Design-Expert software to obtain the optimal parameter combinations and verify the accuracy of the experimental results. The results showed that the optimal reaction conditions were as follows: a catalyst dosage of 2.39%, an isooctanol to dimethyl adipate molar ratio of 2.55 : 1, and a reaction temperature of 117 °C at the time of catalyst addition; this resulted in a high ester exchange rate of 94.23%. Due to the high catalytic efficiency, environmental friendliness and energy saving, and recyclable catalyst, this study provides a feasible process for the effective synthesis of DOA using industrial by-products, which is of significance.

Received 29th November 2024
Accepted 18th February 2025

DOI: 10.1039/d4ra08443h

rsc.li/rsc-advances

1 Introduction

Diisooctyl adipate (DOA) is an excellent cold-resistant plasticizer.[1] It can significantly improve the flexibility of polymers, does not easily change color, and has good water resistance and impact resistance, alongside other characteristics.[2–4] It is widely used in the processing of polyvinyl chloride, vinyl chloride copolymers, polystyrene and other plastics.[5] It is also used as a cold-resistant plasticizer in synthetic rubber, paints and coatings, and as an additive in lubricating oil. In modern industry, the synthesis of DOA is mainly conducted *via* the direct esterification of adipic acid and isooctanol under the action of a catalyst; a large amount of water will be produced in the reaction process, which requires the addition of a water-carrying agent to remove the water.[6] It is necessary to add a water-carrying agent to remove the water to improve the reaction efficiency, however, the water produced as a by-product cannot be reused and can only be discharged as wastewater after proper treatment. Concentrated sulfuric acid, *p*-toluenesulfonic acid, solid acids and other acidic catalysts are widely used in industry. Among them, sulfuric acid, despite its good catalytic effects, strongly corrodes equipment, generates more side reactions, has complicated post-treatment steps, shows low esterification rates during direct esterification reactions, and makes the recovery and utilization of catalysts difficult, causing serious pollution to the environment.[7–12] If it enters water sources, it will also threaten the aquatic ecosystem and human health.[13–15]

In the large-scale production of adipic acid, a large amount of mixed dibasic acid by-product is inevitably generated during the industrial production process.[16,17] This mixed dibasic acid has a complex composition, and mainly contains adipic acid, glutaric acid, and succinic acid.[18,19] So far, it is impossible to separate these directly and effectively *via* physical separation methods.[20] To overcome this problem, researchers have explored an effective solution, methyl esterification distillation, which can easily separate mixed diacids from the mixture as dimethyl esters. Dimethyl adipate is often used as a high-boiling solvent.[21,22] The added value of product utilization is low.

Alkyl titanates are metal titanium organic compounds, which are green and environmentally friendly, with high catalytic activity for esterification and transesterification reactions; however, alkyl titanates are particularly easy to hydrolyze and not easy to separate from reactants. Chelated titanates have

School of Petrochemical Engineering, Shenyang University of Technology, Liaoyang 111003, China. E-mail: 13869119262@163.com; petrochem@126.com; xtjltlt@126.com; Wenruiyang6@163.com; 2093894641@qq.com

significant advantages, such as good stability, not being easy to hydrolyze, needing only mild catalytic reaction conditions, and high selectivity, while they are also non-toxic and harmless, showing great potential for application in organic synthesis, the chemical industry and other fields.

In this study, the chelated titanium adipate catalyst was first prepared from adipic acid and low-carbon alkyl titanates, and the titanium adipate salt was solid. Then, the chelated titanium adipate was used to catalyze the direct transesterification reaction between dimethyl adipate and isooctanol for the synthesis of DOA, and the optimal reaction conditions for the synthesis of DOA were determined using a combination of one-factor and response surface methods. The study not only meets the requirements of green catalysis, easy separation, and recyclability but it also significantly improves the utilization value of dimethyl adipate. Meanwhile, it provides new ideas for related DOA preparation studies and helps to solve existing technical challenges.

2 Materials and methods

2.1 Materials and instruments

2.1.1 Materials. Isopropyl titanate and isooctyl alcohol (analytically pure, Tianjin Fuchen Chemical Reagent Factory); anhydrous ethanol (analytically pure, Tianjin Damao Chemical Reagent Factory); dimethyl adipate (industrial grade, Shandong Jichuang Chemical Co., Ltd); adipic acid (industrial grade, Chongqing Huafeng Chemical Co., Ltd); and dodecylbenzene (industrial grade, Fushun Petrochemical Company) were used.

2.1.2 Analytical instruments and methods. The Fourier transform infrared spectroscopy (FT-IR) instrument was a TENSOR II, Bruker Technology Co., Ltd; the test conditions were as follows: the sample was mixed with KBr and ground, dried and pressed into tablets for testing, and the scanning range was 400–4000 cm^{-1}. The ^{1}H-NMR spectrometer used was an AVANCE, Germany Brooke Technology Co., Ltd; the test conditions were as follows: about 5 mg of sample was fully dissolved in deuterated chloroform ($CDCl_3$) and allowed to stand until it defoamed before testing. The thermogravimetric (TG) analyzer used was a HCT-1, Beijing Hengjiu Scientific Instrument Factory; the test conditions were as follows: 10 mg of sample was placed in a ceramic crucible, and the sample was heated from 20 °C to 800 °C at a rate of 10 °C min^{-1} under a N_2 atmosphere with a gas flow rate of 10 mL min^{-1} to obtain a TG curve. Field-emission scanning electron microscopy (FESEM) was carried out with an Apreo 2C, Seymour Fisher Technologies, Inc., USA; the test conditions were as follows: a small amount of sample was adhered to a conductive adhesive and sprayed with gold. The voltage was 30 kV, the resolution was 500 nm, and the maximum magnification was about 100 000×. The mass spectrometry (MS) analyzer used was a 6540 UHD Q-TOF, Agilent Technologies, USA; the test conditions were as follows: number of injections – 1, injection volume – 20 μL, running time – 1 min.

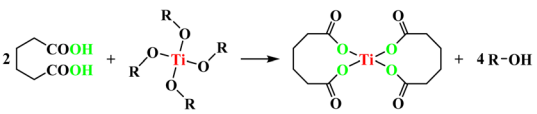

Fig. 1 Preparation of the titanium adipate catalyst.

2.2 Preparation of titanium adipate

7.0 g of adipic acid and 8.0 g of high-temperature solvent were weighed and added into a 150 mL three-necked flask. After stirring and warming up to complete dissolution, 6.8 g of titanate was added dropwise under nitrogen protection and warming was continued; the color of the reaction solution gradually changed from transparent to milky white to a rice-white turbid slurry. The by-product alcohol was evaporated under reduced pressure until no distillate flowed out and the reaction was stopped after 2 h. The reaction product was cooled to room temperature, and the reaction then stopped. The reaction product was transferred to a beaker, washed with anhydrous ethanol three times, and filtered to remove raw materials and solvent that had not completely reacted. The filter cake was dried in a vacuum drier at 90 °C for 3 h to produce a highly active hydrolysis-resistant chelated titanium adipate solid catalyst, as shown in Fig. 1 and 2.

2.3 Synthesis of DOA

In a reaction flask with a stirring device, 5.0 g of dimethyl adipate and 9.3 g of isooctanol were added sequentially under stirring. After heating, when it reached a certain temperature, 2% titanium adipate catalyst (in terms of the total mass of dimethyl adipate + isooctanol) was added, and the temperature of the reaction solution was further elevated until methanol flowed out; the reaction system was then maintained at this

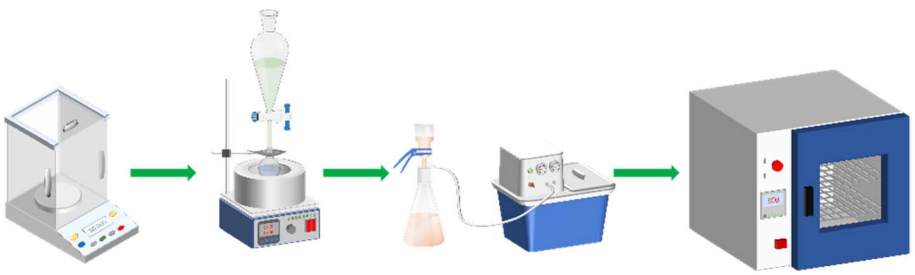

Fig. 2 A diagram of the devices used to prepare the titanium adipate catalyst.

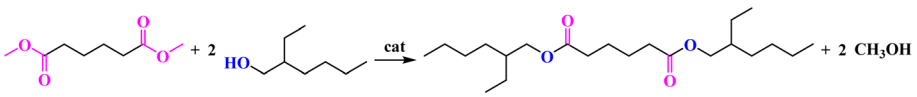

Fig. 3 The synthesis of DOA.

temperature for a certain period. When there was no further obvious outflow of methanol, the temperature of the reaction liquid was gradually increased to remove all methanol and stop the reaction. The by-product methanol was recovered and stored for later use in the methyl esterification of mixed dicarboxylic acid to produce the raw material dimethyl adipate. Subsequently, the reaction solution was transferred to a beaker, and the titanium adipate catalyst in the system was separated *via* hot filtration. The catalyst can be recycled after washing and drying. Then the filtrate was distilled under reduced pressure to evaporate unreacted raw materials and by-products, and finally pure DOA was obtained, as shown in Fig. 3.

In this case, the ester exchange ratio (Y) is calculated as follows (eqn (1)):

$$Y\ (\%) = \frac{m_1}{m_2} \times 100\% \quad (1)$$

where m_1 is the mass of methanol actually produced in the reaction (g) and m_2 is the theoretical mass of methanol (g).

3 Results and discussion

3.1 Catalyst characterization analysis

3.1.1 FT-IR analysis. The fabricated titanium adipate catalyst was subjected to FT-IR testing, as shown in Fig. 4. The absorption peaks at 1719.56 cm^{-1} and 1522.38 cm^{-1} are from –C=O stretching vibration and –C–O bending vibration in –COO–, respectively. The absence of a large broad peak from –OH near 3000 cm^{-1} indicates that the hydroxyl group in –COOH forms coordination bonds with Ti ions. The absorption vibration peaks of Ti–O at 598.50 cm^{-1} and 540.29 cm^{-1} further confirm the successful coordination of titanium with oxygen. In addition, vibrational peaks from $-CH_2$ at 2930.59 cm^{-1} and 2852.95 cm^{-1} were observed. As a result, the product can be initially identified as a titanium adipate catalyst.

3.1.2 TG analysis. The thermal stability of titanium adipate was tested, as shown in Fig. 5. The thermal decomposition of the titanium adipate catalyst mainly consists of two weight-loss intervals, in addition to slight weight loss below 170 °C due to a small amount of water and solvent attached to the sample: between 170 and 457 °C, the Ti–O bonds are broken and continuously oxidized, and the complex loses weight drastically; the weight loss in the interval of 457–580 °C is due to the combustion of residual carbon in the titanium adipate, and the final product is TiO_2. The overall weight loss of the titanium adipate product was calculated to be 70.03%, which was consistent with the theoretical weight loss, and further proved that the product was the target product aimed to be synthesized.

3.1.3 Scanning electron microscopy. The morphology and elemental composition of titanium adipate were analyzed, and it can be seen from Fig. 6(a) that titanium adipate consists of smooth spherical particles of uniform size, with a concentrated size distribution in the range of 1.5–2.0 μm. According to the EDS images shown in Fig. 6(b–e), the Ti, O, and C elements were uniformly distributed on the surface of the titanium adipate catalyst, and the mass fractions of these elements were 38.11%, 31.60%, and 30.28%, respectively.

The morphology and elemental composition of titanium adipate recovered after use were analyzed, and it can be seen from Fig. 7(a) that the morphology of the recovered titanium adipate changed little; it was still made up of spherical-like particles. According to the EDS analysis shown in Fig. 7(b–e),

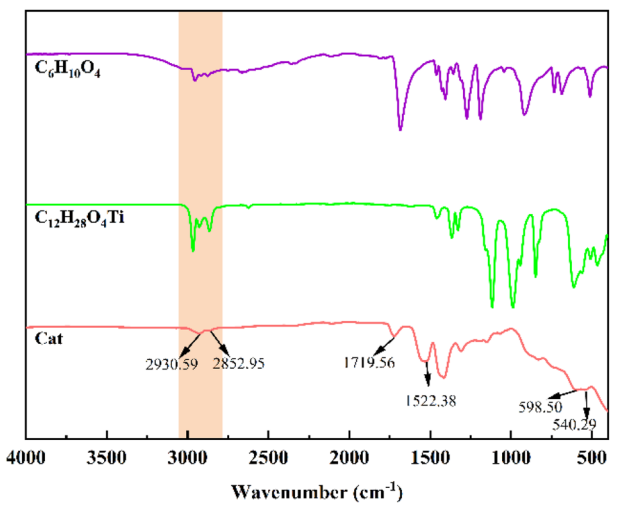

Fig. 4 The FT-IR spectrum of titanium adipate (Cat), with adipic acid and titanate shown for reference.

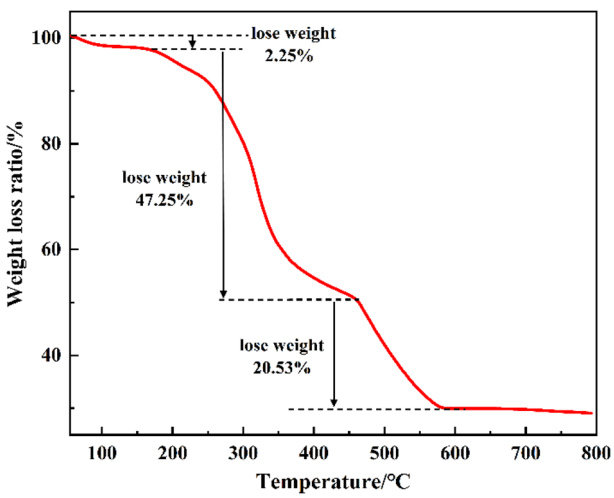

Fig. 5 TG analysis of titanium adipate.

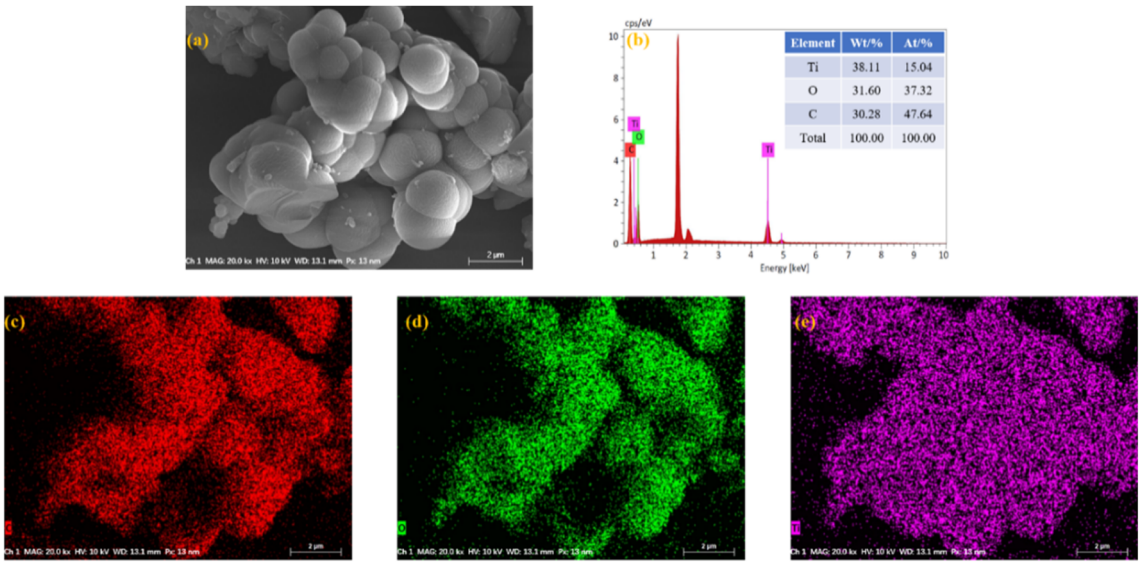

Fig. 6 (a) An FESEM photograph and (b–e) EDS analysis of titanium adipate.

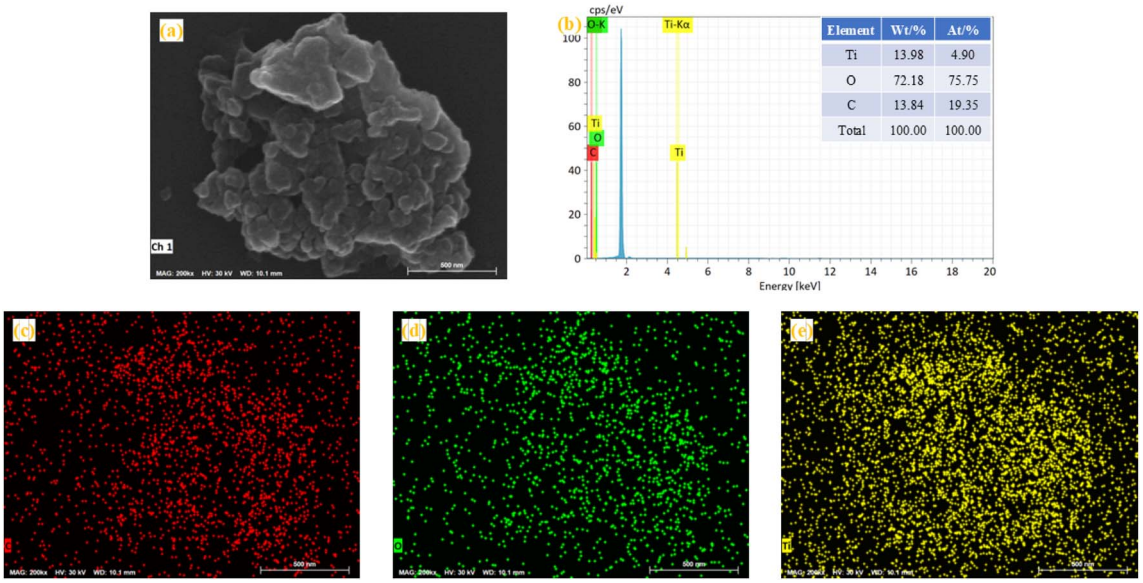

Fig. 7 (a) An FESEM photograph and (b–e) EDS analysis of recovered titanium adipate.

the Ti, O and C elements were evenly distributed on the surface of the catalyst, while the Ti and C elemental mass fractions decreased.

3.2 Characterization and analysis of diisooctyl adipate

3.2.1 FT-IR analysis. The products obtained from the titanium-adipate-catalyzed transesterification reaction were characterized using FT-IR, and the results are shown in Fig. 8. It can be stated that the peak at 1730.51 cm^{-1} is the C=O condensation vibrational absorption peak,[23] and those at 2957.41 cm^{-1} and 2929.10 cm^{-1} are attributed to the asymmetric stretching vibrational absorption peaks of $-CH_3$ and $-CH_2$, respectively.[24] The peaks at 2873.23 cm^{-1} and 2859.45 cm^{-1} are attributed to $-CH_3$ and $-CH_2$ -symmetric stretching vibrational absorption peaks, respectively. The peak at 1459.88 cm^{-1} is attributed to the C–H bond deformation vibration absorption peaks.[23] No –OH absorption peaks or absorption peaks from other substances appeared, indicating that there are no raw materials, water or other substances in the product; it can be initially deduced that the obtained product is high-purity DOA.

3.2.2 ^{1}H-NMR characterization analysis. To further determine the structure of the product, it was characterized *via* ^{1}H-NMR, and the results are shown in Fig. 9. The obtained spectral data are as follows – ^{1}H NMR (400 MHz, $CDCl_3$): δ 3.93 (dtt, J = 8.8, 6.2, 2.9 Hz, 4H), 2.35–2.22 (m, 4H), 1.89 (qd, J = 8.9, 2.7 Hz, 2H), 1.66–1.51 (m 2H), 1.22 (q, J = 6.1 Hz, 16H), 0.86–

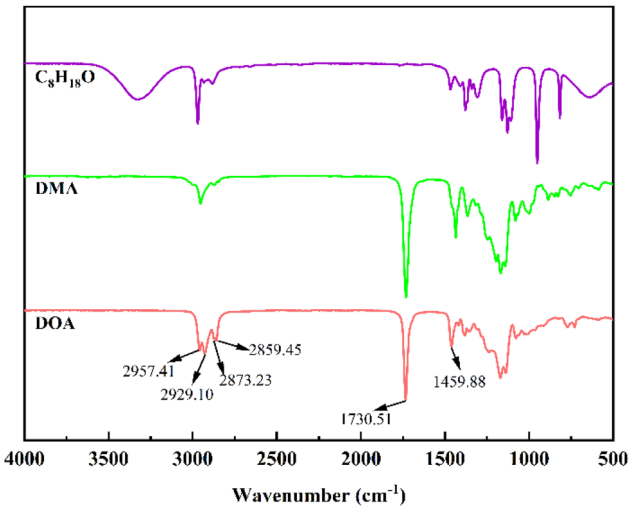

Fig. 8 The FT-IR spectrum of DOA, with DMA and isooctanol shown for reference.

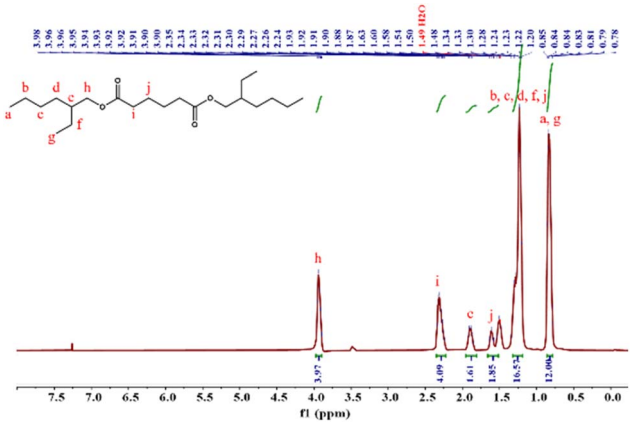

Fig. 9 ^{1}H-NMR analysis of DOA.

0.78 (m, 12H). Upon analyzing the number and species of H atoms and combining this with FT-IR spectral analysis, the synthesized product can be identified as DOA.

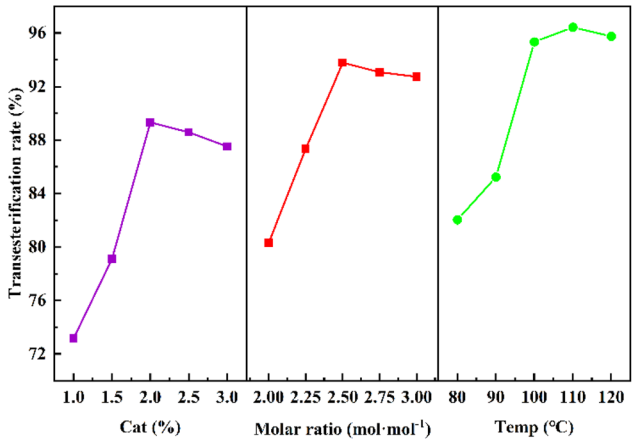

Fig. 11 Effects of different factors on the ester exchange rate.

3.2.3 Mass spectrometry analysis. The mass spectral characterization of the synthesized DOA is shown in Fig. 10. The relative molecular mass of DOA is 370.57, and Fig. 10 shows an MS peak at *m*/*z*: 393.31 $\{[M + Na]^{+}\}$, indicating that the synthesized product is DOA.

3.3 Effects of factors on the esterification rate

In general, the factors influencing a transesterification reaction include the reactant molar ratio, catalyst dosage, reaction temperature, temperature upon catalyst addition, and reaction time. In this experiment, the controllable main influencing factors are the reactant molar ratio, catalyst dosage, and temperature upon catalyst addition. In this regard, the effects of catalyst dosage (1.0%, 1.5%, 2.0%, 2.5%, and 3.0%), reactant molar ratio (2.00 : 1, 2.25 : 1, 2.50 : 1, 2.75 : 1, and 3.00 : 1), and reaction temperature at the time of catalyst incorporation (80 °C, 90 °C, 100 °C, 110 °C, and 120 °C) on the transesterification rate were investigated in this study. The results are shown in Fig. 11.

It can be seen from Fig. 11 that the ester exchange rate initially increased with an increase in catalyst dosage, indicating that the titanium adipate catalyst has a good catalytic effect on this reaction. When the catalyst dosage was increased to 2.0%, the number

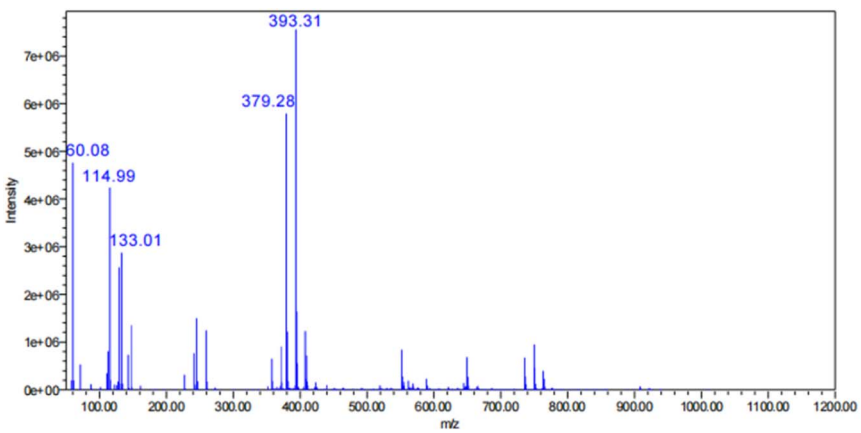

Fig. 10 The mass spectrum of DOA.

Table 1 Response surface test factors and level design

		Coded levels		
Independent variable	Unit	−1	0	1
A: reaction temperature when the catalyst is added	°C	100	110	120
B: catalyst amount	%	1.5	2.0	2.5
C: raw material alcohol:ester molar ratio	mol mol^{-1}	2.25	2.50	2.75

Table 2 Response surface test design and results

Number	*A*	*B*	*C*	Ester exchange ratio/%
1	100	2.0	2.75	93.02
2	110	2.0	2.50	93.35
3	120	2.0	2.25	90.12
4	110	2.5	2.75	94.16
5	110	1.5	2.25	80.84
6	120	2.5	2.50	94.78
7	120	1.5	2.50	89.78
8	110	1.5	2.75	89.95
9	100	2.0	2.25	83.93
10	100	1.5	2.50	84.49
11	100	2.5	2.50	92.35
12	110	2.0	2.50	92.96
13	110	2.5	2.25	92.89
14	110	2.0	2.50	92.57
15	120	2.0	2.75	94.58

of side reactions increased, resulting in a decrease in the ester exchange rate. The effect of the molar ratio of reactants on the transesterification reaction showed a similar trend; within a certain range, increasing the dosage of isooctanol was favorable to the reaction, and when n(isooctanol) : n(dimethyl adipate) = 2.50 : 1, the transesterification rate reached 93.77%. Upon continuing to increase the dosage of isooctanol, the concentration of the reaction system decreased, which led to a gradual decrease in the yield. When the catalyst addition temperature was low, the activation energy of the reactant molecules was low, and the catalytic effect of the catalyst was not obvious. As the temperature increases, the activation energy of the reactant molecules increases, and the catalyst can reduce the activation energy of the reaction more effectively. However, when the addition temperature is too high, the catalyst may undergo physical or chemical changes, resulting in a decrease in its activity.

At a catalyst dosage of 2%, a reactant molar ratio of 2.5 : 1, and a catalyst addition temperature of 110 °C, the ester exchange rate reached relatively high values; this provided coded-level central values for the establishment of the response surface below.

3.4 Response surface optimization

3.4.1 Response surface experimental design and results. Response surface methodology is used to study the quantitative relationship between independent variables and response variables and to evaluate the effects of independent variables and their interactions on the response variables by designing experiments and establishing mathematical models, and it is commonly used to optimize the conditions of chemical reactions and to improve the process flow.[25,26] To deeply investigate the effects of the interactions among factors on the ester exchange rate, response surface experiments were applied in this study to optimize the relevant parameters. According to the principles of Box–Behnken central combinatorial design, a 3-factor, 3-level response surface analysis experiment was designed, with reaction temperature (A), catalyst dosage (B) and molar ratio of reactants (C) as the independent variables, and the ester exchange rate (Y) as the response value; the

Table 3 Regression model significance testing[a]

Source	Sum of squares	df	Mean square	*F*-value	*P*-value	Significance
Model	252.52	9	28.06	46.68	0.0003	Significant
A	29.92	1	29.92	49.77	0.0009	
B	106.00	1	106.00	176.34	< 0.0001	
C	71.58	1	71.58	119.09	0.0001	
AB	2.04	1	2.04	3.40	0.1244	
AC	5.36	1	5.36	8.92	0.0306	
BC	15.37	1	15.37	25.56	0.0039	
A^2	2.54	1	2.54	4.22	0.0952	
B^2	11.72	1	11.72	19.49	0.0069	
C^2	10.91	1	10.91	18.15	0.0080	
Residual	3.01	5	0.6011			
Lack of fit	2.70	3	0.9004	5.92	0.1479	Not significant
Pure error	0.3042	2	0.1521			
Cor total	255.53	14				
R^2	0.9882		C.V.%	0.8553		
Adjusted R^2	0.9671		Adeq. precision	22.6531		

[a] $0.01 < P < 0.05$ – significant; $P < 0.01$ – very significant.

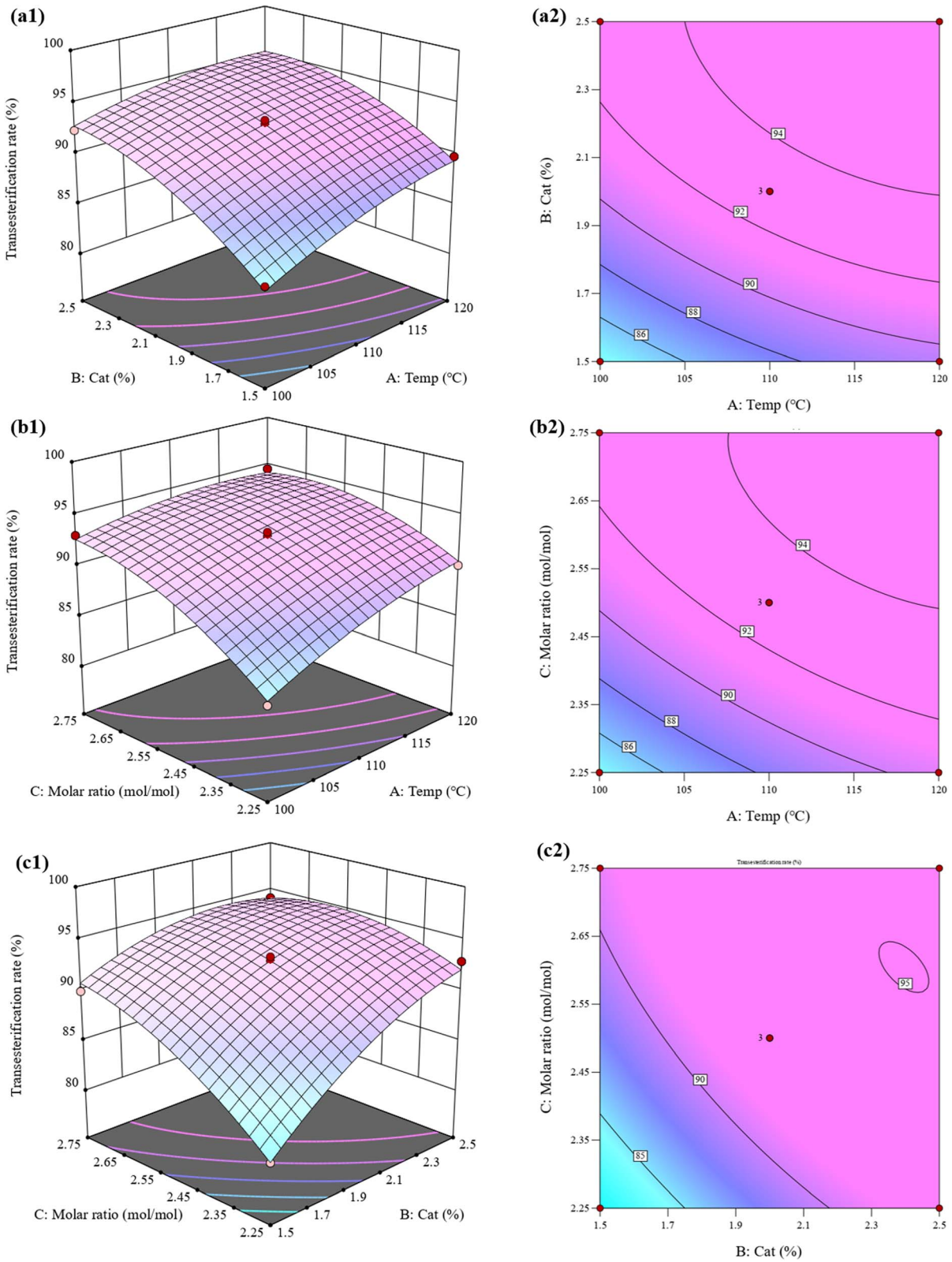

Fig. 12 Response surface plots and contour plots of the response surface for optimizing the ester exchange rate: (a) reaction temperature and catalyst dosage; (b) reaction temperature and reactant molar ratio; and (c) catalyst dosage and reactant molar ratio.

experimental factor levels and coding are shown in Table 1.[27,28] A total of 15 sets of experiments were run for the response surface design, and the results are shown in Table 2.

3.4.2 Model building and significance test. Based on the experimental results in Table 2, a quadratic-fit regression equation (eqn (2)) showing the relationship between the response value and the 3 factors was established using Design-Expert software:[29–33]

$$Y(\text{ester exchange ratio}) = 92.96 + 1.93A + 3.64B + 2.99C - 0.715AB - 1.16AC - 1.96BC - 0.8287A^2 - 1.78B^2 - 1.72C^2 \quad (2)$$

It can be seen that eqn (2) has great value and can be optimized for the parameters involved. To further examine the significance of the model, the simulated regression equation was subjected to ANOVA and significance test, and the results are shown in Table 3.

As shown in Table 3, the model *P*-value of 0.0003 is less than 0.01, indicating that the model as a whole has good significance and regressivity. By analyzing the *F*-values, it can be determined that the three factors affect the model in the following order of importance: the catalyst dosage is the most significant, followed by the molar ratio of the reactants, and lastly, the reaction temperature at the time of catalyst addition. The lack-of-fit term of the model has a *P*-value of 0.1479, which is greater than 0.05, indicating that the lack-of-fit of the response values is not significant and that the model suitably describes the relationship between the independent variables and the response value. In addition, the correlation coefficient of the model, R^2, is 0.9882, the adjusted coefficient of determination, $R_{Adj}{}^2$, is 0.9671, and the coefficient of variation, C.V., is 0.8553%, which is less than 10%, indicating that it has a sufficiently strong signal and the model is ideal.

3.4.3 Interaction analysis. Response surface and contour plots provide a visual way to observe the effects of factors on the results and their interactions, where the steepness of the response surface reflects the degree of influence of a single factor on the results. The response surface and contour plots of the effects of reaction temperature, catalyst dosage, and reactant molar ratio on the ester exchange rate at the time of catalyst addition are shown in Fig. 12.

Combining Fig. 12(a1) and (a2), it can be seen that the transesterification rate is less than 80% when the catalyst dosage is low and the addition temperature is low, but with an increase in dosage and temperature, the yield can be increased to more than 95%. Combining Fig. 12(b1) and (b2), it can be seen that the transesterification rate becomes higher and higher with the elevation of the alcohol: ester molar ratio and the catalyst addition temperature. Combining Fig. 12(c1) and (c2), it can be seen that with an increase in the alcohol: ester molar ratio and catalyst dosage, the ester exchange rate also showed an increasing trend, and the effects of the three factors on the ester exchange rate were positively correlated. Among them, the interaction of the alcohol:ester molar ratio and catalyst dosage had the greatest effect on the ester exchange rate, and the interaction of the alcohol:ester molar ratio and catalyst addition temperature had the second greatest effect on the ester exchange rate.

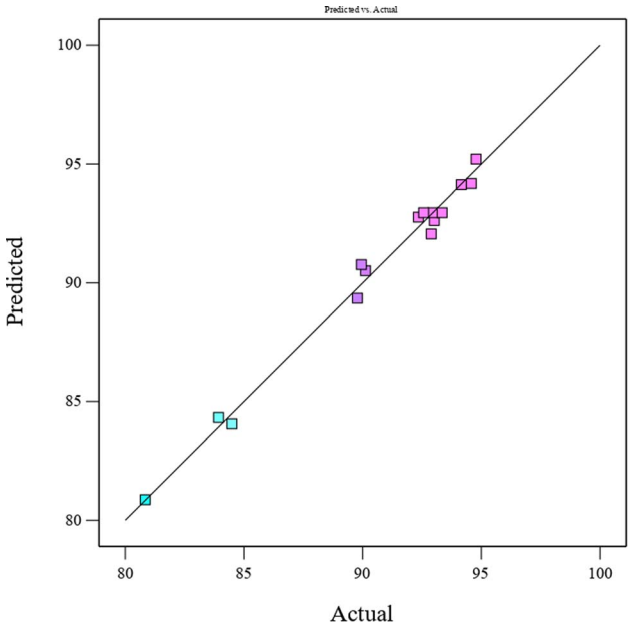

Fig. 13 A comparison of the experimental results with the model-predicted DOA yields.

3.4.4 Box–Behnken model adequacy checking. Usually, model adequacy testing, as part of model validation, is essential in verifying the accuracy of a model and validating the analysis of experimental data. A valid and accurate mathematical model will provide an adequate approach to the actual process. Fig. 13 shows a comparison between the experimental results and the model-predicted ester exchange rate; this clearly shows that the data points are uniformly distributed near the fitted straight line, the predicted and experimental values present a high degree of agreement, and the experimental values have good fit.[34] The maximum ester exchange rate (*Y*) value was taken to be the optimization target, and multiple regression fitting analysis was conducted to determine the optimal reaction conditions, which are as follows: a catalyst dosage of 2.38827%, a temperature at catalyst addition of 116.961 °C, and a molar ratio of reactants of 2.5482 : 1; the model response value under these conditions was 95.3345%. For the convenience of practical operation, the optimal process conditions were modified: the catalyst dosage was 2.39%, the catalyst temperature was 117 °C, and the reactant molar ratio was 2.55 : 1. Under these conditions, three sets of repeat validation tests were conducted; the average ester exchange rate obtained in the tests was 94.23%, and the relative error of the predicted value was −1.1045%, which indicated that the results of this model were reliable and had excellent predictive ability.[28,35]

3.5 Catalyst reuse effects

The reaction was carried out under the optimal conditions. At the end of the reaction, the catalyst was filtered and separated,

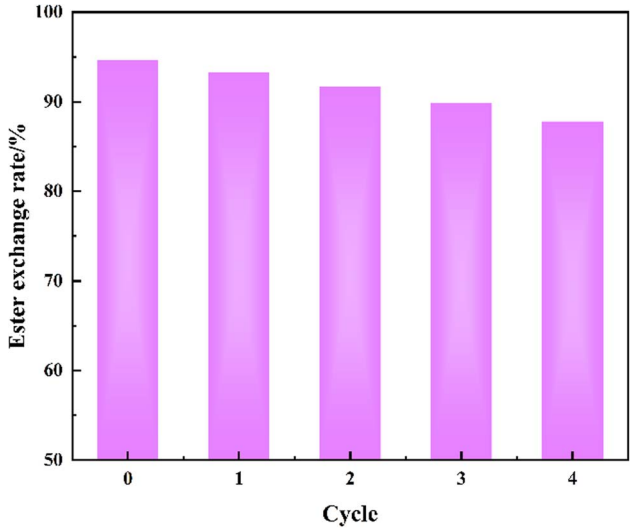

Fig. 14 Effects of the reuse of the catalyst.

washed and dried with anhydrous ethanol, and used repeatedly to study the service life of the catalyst. The results are shown in Fig. 14.

It is obvious from Fig. 14 that the ester exchange rate decreased when the catalyst was reused, but the decrease was not obvious, and the ester exchange rate was still above 85% after four cycles of recycling. Therefore, the catalyst prepared in this study has high activity and stability and can be reused.

4 Conclusions

Novel titanium adipate catalysts, which are non-toxic and harmless, with high catalytic activity and thermal stability, were prepared *via* an exchange reaction using titanate and adipic acid as raw materials. The prepared titanium adipate catalysts had a regular spherical structure with uniform size.

Titanium adipate was used to catalyze the ester exchange reaction for the synthesis of diisooctyl adipate, and the effects of factors such as the reaction temperature, catalyst dosage, and alcohol to ester molar ratio at the time of catalyst addition on the ester exchange reaction were investigated. Based on one-way experiments, response surface methodology was used to optimize the reaction conditions for the synthesis of DOA, and the optimal process conditions were obtained as follows: a catalyst dosage of 2.39%, a catalyst addition temperature of 117 °C, and a molar ratio of the reactants isooctanol to dimethyl adipate of 2.55 : 1. Validation experiments were carried out several times under these experimental conditions, and the average yield of DOA obtained was 94.23%, which was similar to that predicted by the model. As the titanium adipate catalyst is solid, it is easy to separate from the product and can be reused many times without impurities in the product. The method creates little environmental pollution, uses mild reaction conditions, is simple to operate, can effectively reduce production costs, and meets the requirements of green chemistry; thus, it has good prospects for industrial application.

Data availability

All data supporting the findings of this study are presented in the article.

Author contributions

Guoliang Shen and Tiejun Xu conceived, planned and supervised the experiment. Linlin Zhao and Ruiyang Wen were responsible for the main part of the experiment, including the preparation of catalysts and the synthesis of DOA. Ruiyang Wen and Sijin Jiang were responsible for the characterization and analysis of the catalyst. Linlin Zhao and Sijing Jiang wrote the first draft of the manuscript, and all the authors reviewed the manuscript.

Conflicts of interest

The authors declare that they have no conflicts of interest.

Acknowledgements

Thanks to all the authors for their efforts in completing this manuscript.

Notes and references

1 W. Fletcher, A. Gent and R. Wood, *Rubber Chem. Technol.*, 1957, **30**, 652–666.
2 H.-J. Kim, Y. Kwon and C. K. Kim, *J. Nanosci. Nanotechnol.*, 2013, **13**, 577–581.
3 X. Li, X. Nie, J. Chen and Y. Wang, *Polym. Int.*, 2017, **66**, 443–449.
4 V. Najafi and H. Abdollahi, *Eur. Polym. J.*, 2020, **128**, 109620.
5 Z. Y. Guo, P. P. Gai, J. Duan, J. X. Zhai, S. S. Zhao, S. Wang and D. Y. Wei, *Biomed. Chromatogr.*, 2010, **24**, 1094–1099.
6 A. Sahu and A. B. Pandit, *Ind. Eng. Chem. Res.*, 2019, **58**, 2672–2682.
7 A. H. M. Fauzi and N. A. S. Amin, *Energy Convers. Manage.*, 2013, **76**, 818–827.
8 N. Muhammad, Y. A. Elsheikh, M. I. A. Mutalib, A. A. Bazmi, R. A. Khan, H. Khan, S. Rafiq and Z. Man, *J. Ind. Eng. Chem.*, 2015, **21**, 1–10.
9 P. Fan, S. Xing, J. Wang, J. Fu, L. Yang, G. Yang, C. Miao and P. Lv, *Fuel*, 2017, **188**, 483–488.
10 Y. Feng, T. Qiu, J. Yang, L. Li, X. Wang and H. Wang, *Chin. J. Chem. Eng.*, 2017, **25**, 1222–1229.
11 A. P. da Luz Corrêa, R. R. C. Bastos, G. N. da Rocha Filho, J. R. Zamian and L. R. V. da Conceição, *RSC Adv.*, 2020, **10**, 20245–20256.
12 D. Procopio and M. L. Di Gioia, *Catalysts*, 2022, **12**, 50.
13 X. Xu, S. Zhang, Y. Wang, N. Wang, Q. Jiang, X. Liu, Q. Guan and W. Zhang, *Appl. Catal., B*, 2024, **345**, 123701.
14 N. Wang, Z. Zhang, Y. Zhang, X. Xu and Q. Guan, *Sep. Purif. Technol.*, 2025, **355**, 129566.
15 Z. Shan, Y. Yang, H. Shi, J. Zhu, X. Tan, Y. Luan, Z. Jiang, P. Wang and J. Qin, *Front. Chem.*, 2021, **9**, 755836.

16 P. Vogtel and G. Steinhoff, Process for the recovery of adipic acid, *US Pat.*, 5264624, 1993.
17 J. Lu, H. Chen, Y. Huang, L. Zhang, Z. Zhao, W. Du and X. Wang, *Fluid Phase Equilib.*, 2019, **485**, 1–15.
18 B. C. Sutradhar, Crystallization of adipic acid from its solution in aqueous nitric acid, *US Pat.*, 6946572, 2005.
19 F. Wang, Y. Li, Z. Ning, C. Jiang and X. Wang, *J. Chem. Eng. Data*, 2016, **61**, 3059–3068.
20 R. Li, L. Lin, W. Feng, J. Xu, C. Du and H. Zhao, *J. Chem. Thermodyn.*, 2017, **107**, 8–17.
21 A. M. Silva, M. A. Morales, E. M. Baggio-Saitovitch, E. Jordao and M. A. Fraga, *Appl. Catal., A*, 2009, **353**, 101–106.
22 A. Gorak and A. Stankiewicz, *Annu. Rev. Chem. Biomol. Eng.*, 2011, **2**, 431–451.
23 Y. Sun, Y. Yan, X. Zheng, J. Han, B. Wang, Q. Wu and G. Bai, *Mol. Catal.*, 2024, **553**, 113732.
24 Z. Fu, K. Shi, F. Ma, R.-m. Song, L. Chen, J.-s. Dai and W.-q. Shen, *Int. J. Pavement Eng.*, 2022, **23**, 2644–2653.
25 A. K. Domingos, E. B. Saad, H. M. Wilhelm and L. P. Ramos, *Bioresour. Technol.*, 2008, **99**, 1837–1845.
26 Y. Kim, M. Kim, J. Hwang, E. Im and G. D. Moon, *Polymers*, 2022, **14**, 656.
27 R. Wen, G. Shen, J. Zhai, L. Meng and Y. Bai, *New J. Chem.*, 2023, **47**, 14646–14655.
28 R. Wen, G. Shen, M. Zhang, Y. Yu and S. Xu, *New J. Chem.*, 2024, **48**, 17254–17260.
29 N. Altunay, Y. Unal and A. Elik, *Food Addit. Contam.,: Part A*, 2020, **37**, 869–881.
30 C. Fanali, V. Gallo, S. Della Posta, L. Dugo, L. Mazzeo, M. Cocchi, V. Piemonte and L. De Gara, *Molecules*, 2021, **26**, 2652.
31 P. Yu, Q. Li, Y. Feng, S. Ma, Y. Chen and G. Li, *Molecules*, 2021, **26**, 1310.
32 Y.-T. Ao, Y.-C. Chen and W.-H. Ding, *J. Hazard. Mater.*, 2021, **401**, 123383.
33 C. Xing, W.-Q. Cui, Y. Zhang, X.-S. Zou, J.-Y. Hao, S.-D. Zheng, T.-T. Wang, X.-Z. Wang, T. Wu and Y.-Y. Liu, *Ultrason. Sonochem.*, 2022, **83**, 105946.
34 M. Shahedi, Z. Habibi, M. Yousefi, J. Brask and M. Mohammadi, *Int. J. Biol. Macromol.*, 2021, **170**, 490–502.
35 P. Chen, X. Liu, L. Wang, C. Wang and J. Fu, *J. Sep. Sci.*, 2021, **44**, 585–599.